One simple explanation of the extreme matrix dependence of $k(T)$ for $Cr(NH_3)_5Cl^{2+}$ is that more relaxation channels are available in the DMSO/0.1 M HCl glass than in the doped crystalline solid (alternatively, the BISC channel would have to involve a large solvent contribution). If only the BISC channel were available in the doped solid, our estimate of $\Delta E_{DQ} \geq 6.8$ kcal mol^{-1} (or 2.4×10^3 cm^{-1} as in Table III) suggests that, in the solid, E_a(estd) $\geq$ 6.8 kcal mol^{-1} + $E_{a,Q}$. This can be compared to E_a(obsd) = 6.9 kcal mol^{-1}.

If several (N_c) channels do contribute to (^{2}E)Cr(III) relaxation in solution, then

$$k(T) = \sum_{i=1}^{N_c} k_i(T) = \sum_{i=1}^{N_c} A_i \exp(-\Delta G_i^{\ddagger}/RT)$$

where the sum extends over all possible relaxation channels. In such an event, "average" values of E_a(obsd) and A(obsd) would be obtained from the data fits. If the temperature independent component of $k(T)$ is represented by an effective entropy of activation, $\Delta S^{\ddagger}_{eff}$ will be larger in the multiple channel situation than the average of the entropies of activation ($\Delta S_i^{\ddagger}$ for the individual channels: $\Delta S^{\ddagger}_{eff} > (\sum_{i=1}^{N_c} \Delta S_i^{\ddagger})/N_c$). This effect could be one factor contributing to exceptionally large preexponential factors characteristic of the compounds with $T_{tr} < 200$ K.

We have long been concerned with the very large Arrhenius preexponential factors (10^{15}–10^{22} s^{-1}) of $k(T)$ found for many of these compounds.[2d,g,h] Somewhat smaller but still large values (10^{13}–10^{15} s^{-1}) are commonly found for many compounds in fluid solution. These preexponential factors do vary with the solvent matrix.[2d,g,h] The exceptionally large values, $A > 10^{18}$ s^{-1} are nearly all obtained in glassy matrices, and they are very likely related to a distribution of solvation environments, each with a different fluidity, melting range, etc. In such a situation the inferred values of $\Delta S^{\ddagger}_{eff}$ must be large, partly for reasons described in the previous paragraph.

Summary and Conclusions

We have compared the photophysical behavior of several stereochemically constrained chromium(III)–macrocyclic ligand complexes to that of simpler ammine complexes. The results indicate that several relaxation mechanisms are important among these complexes. In particular, the relaxation channel, which is sensitive to macrocyclic ligand stereochemistry in ammine and cyano complexes, does not appear to dominate the ^{2}E excited-state relaxation of complexes containing the chloride or bromide ligands. Rather these halo complexes relax by means of a stereochemically insensitive pathway that may involve back intersystem crossing to populate the lowest energy quartet excited state.

Contribution from the Department of Applied Chemistry, Faculty of Engineering, Kumamoto University, Kurokami, Kumamoto 860, Japan

Ab Initio MO Study of CO_2 Insertion into a Cu(I)–H Bond. Semiquantitative Understanding of Changes in Geometry, Bonding, and Electron Distribution during the Reaction

Shigeyoshi Sakaki* and Katsutoshi Ohkubo

Received September 29, 1988

An ab initio MO study was carried out on CO_2 insertion into a Cu(I)–H bond of $CuH(PH_3)_n$ (n = 2, 3). $Cu(PH_3)_2(\eta^2\text{-}O_2CH)$ is predicted to be a final product in the reaction of $CuH(PH_3)_2$, while in the reaction of $CuH(PH_3)_3$, $Cu(PH_3)_3(\eta^1\text{-}OCOH)$ is predicted to be a final product. In both reaction systems, the CO_2 insertion is calculated to be significantly exothermic and its activation barrier is estimated to be rather small, which suggests the CO_2 insertion into the Cu(I)–H bond is facile. Around the transition state, the $CuH(PH_3)_2$ moiety is distorted little but the CO_2 moiety is somewhat distorted. The origin of the activation barrier is the destabilization due to the CO_2 distortion and the exchange repulsion between $CuH(PH_3)_2$ and CO_2. The destabilization arising from these factors is compensated by a strong charge-transfer interaction from $CuH(PH_3)_2$ to CO_2 and an electrostatic attraction between $Cu^{\delta+}$ and $O^{\delta-}$ of CO_2. This is the reason that the activation barrier is rather small. Through this theoretical study, we obtained a useful guideline to finding a metal complex that easily causes the CO_2 insertion.

Introduction

There has been much current interest in the interaction of CO_2 with transition-metal complexes, since formation of transition-metal complexes is one of the most powerful and universal ways of activating inert molecules.[1] Several transition-metal complexes capable of reacting with CO_2 have been known.[1] For instance, CO_2 easily coordinates with $IrCl(dmpe)_2$ (dmpe = $Me_2PCH_2CH_2PMe_2$), by which electrophilic attack on the O atom is significantly accelerated.[2] Also, CO_2 inserts into an M–X bond (X = H^-, CH_3^-, OR^-) of metal complexes, such as Co(I),[3] Cu(I),[4,5] Rh(I),[6] Ru(II),[7] Ru(0),[8] Al(III),[9] Cr(0), Mo(0), and W(0),[10,11] Ni(II),[12] Mo(VI),[13] Zn(II),[14] and In(III)[15] complexes. However,

Chart I

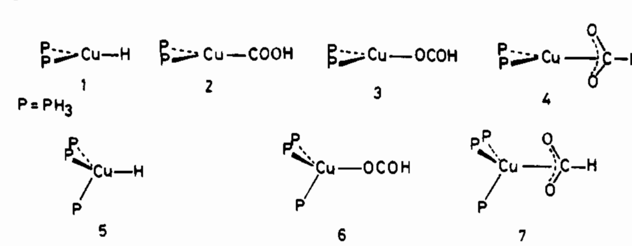

(1) See for example: (a) Inoue, S., Yamazaki, N., Eds. *Organic and Bioorganic Chemistry of Carbon Dioxide*; Kodansha: Tokyo, 1983. (b) Darenbourg, D. J.; Kudaroski, R. A. *Adv. Organomet. Chem.* **1983**, *22*, 129. (c) Palmar, D. A.; Van Eldik, R. *Chem. Rev.* **1983**, *83*, 651. (d) Walther, D. *Coord. Chem. Rev.* **1987**, *79*, 135.
(2) (a) Harlow, R. L.; Kinney, J. B.; Herskovitz, T. *J. Chem. Soc., Chem. Commun.* **1980**, 813. (b) Calabrese, J. C.; Herskovitz, T.; Kinney, J. B. *J. Am. Chem. Soc.* **1983**, *105*, 5914. (c) Forschner, T.; Menard, K.; Cutler, A. *J. Chem. Soc., Chem. Commun.* **1984**, 121.
(3) Pu, L. S.; Yamamoto, A.; Ikeda, S. *J. Am. Chem. Soc.* **1968**, *90*, 3896.
(4) (a) Miyashita, A.; Yamamoto, A. *J. Organomet. Chem.* **1973**, *49*, C57. (b) Ikariya, T.; Yamamoto, A. *J. Organomet. Chem.* **1974**, *72*, 145. (c) Tsuda, T.; Chujo, Y.; Saegusa, T. *J. Am. Chem. Soc.* **1978**, *100*, 632. (d) Beguin, B.; Denise, B.; Sneeden, R. P. A. *J. Organomet. Chem.* **1981**, *208*, C18.
(5) Bianchini, C.; Ghilardi, C. A.; Meli, A.; Midollini, S.; Orlandini, A. *Inorg. Chem.* **1985**, *24*, 924.

all these reactions are not catalytic but stoichiometric. It seems still difficult to find a good transition-metal complex that reacts with CO_2 and performs catalytic CO_2 fixation into organic substances, except for a few of pioneering works[16] and a number of electrocatalytic reductions of CO_2.[17] Some of the catalytic CO_2 fixations are expected to involve CO_2 insertion or electrophilic attack on CO_2 as a key elementary process. Therefore, theoretical investigation of those processes should be helpful in providing us with some meaningful information about CO_2 fixation.

In the past decade, several MO studies have been carried out on transition-metal CO_2 complexes.[18-21] However, the coordinate-bond nature of CO_2 and stereochemistry of CO_2 complexes have been mainly discussed in those studies and very little has been theoretically reported about CO_2 conversion into organic substances, except for only our preliminary work.[22]

In the present work, CO_2 insertion into a metal–hydride bond is theoretically investigated with the ab initio MO/MP2 method. CO_2 insertion into a Cu(I)–H bond of $CuH(PH_3)_2$ (**1**) and $CuH(PH_3)_3$ (**5**) is chosen as a model (see Chart I for these complexes), because CO_2 insertion into the Cu(I)–alkyl and Cu(I)–H bonds is well-known.[4,5,23] In the CO_2 reaction with **1**, three compounds $Cu(PH_3)_2(\eta^1\text{-COOH})$ (**2**), $Cu(PH_3)_2(\eta^1\text{-OCOH})$ (**3**), and $Cu(PH_3)_2(\eta^2\text{-}O_2CH)$ (**4**) are examined as possible products. In the reaction with **5**, two compounds $Cu(PH_3)_3(\eta^1\text{-OCOH})$ (**6**) and $Cu(PH_3)_3(\eta^2\text{-}O_2CH)$ (**7**) are investigated as possible products. In this case, $Cu(PH_3)_3(\eta^1\text{-COOH})$ is excluded from discussion, because the same type of compound **2** is calculated to be much less stable than **3** and **4** and furthermore the lesser stability of the M–COOH type compound is considered to be common in Cu(I) complexes, as described below. Through this theoretical work, we hope (a) to investigate the thermodynamics of the CO_2 insertion into the Cu(I)–H bond, (b) to estimate its activation barrier and to clarify the origin of the activation barrier, and (c) to elucidate how and why geometry and electronic structure (bonding and electron distribution) change during the reaction. It is our intention with this work to provide the first detailed theoretical information of the CO_2 insertion into the metal–hydride bond that should help to find good transition-metal complexes for catalytic CO_2 fixation.

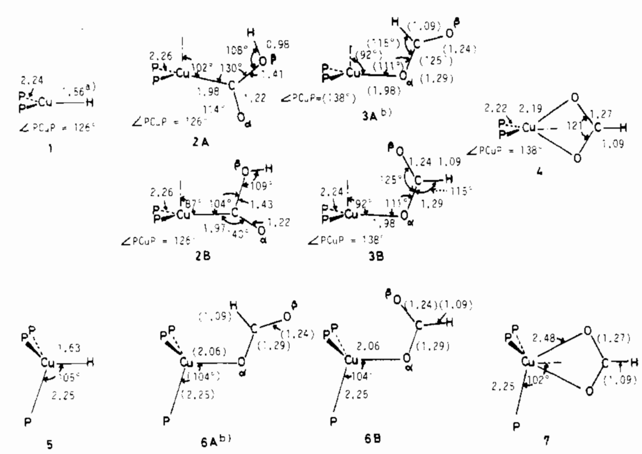

Figure 1. Optimized geometrical parameters of various Cu(I) complexes (assumed values in parentheses): (a) R(Cu–H) = 1.60 Å, when full geometry optimization was carried out; (b) the assumed structure used for calculations (see text).

Table I. Relative Stabilities of Products of CO_2 Insertion (kcal/mol)

compd	no.	BS I HF	BS II HF	BS II MP2	BS III HF
$CuH(PH_3)_2$ (**1**) + CO_2		0.0[a]	0.0[b]	0.0[c]	0.0[d]
$Cu(\eta^1\text{-COOH})(PH_3)_2$	**2A**	−6.2	−16.5	−13.8	−19.4
	2B	−15.5	−22.8	−19.8	−26.1
$Cu(\eta^1\text{-OCOH})(PH_3)_2$	**3A**	−24.8	−26.4	−16.7	−41.2
	3B	−39.0	−40.2	−29.0	−55.6
$Cu(\eta^2\text{-}O_2CH)(PH_3)_2$	**4**	−38.9	−37.5	−29.1	−56.8
$CuH(PH_3)_3$ (**5**) + CO_2		0.0[e]	0.0[f]	0.0[g]	0.0[h]
$Cu(\eta^1\text{-OCOH})(PH_3)_3$	**6A**	−29.0	−29.0	−17.9	−45.5
	6B	−40.9	−41.7	−28.2	−59.3
$Cu(\eta^2\text{-}O_2CH)(PH_3)_3$	**7**	−34.1	−36.1	−18.1	−57.0

[a] E_t = −704.9539 for $CuH(PH_3)_2$ and −187.1729 for CO_2. [b] E_t = −727.7275 for $CuH(PH_3)_2$ and −187.5530 for CO_2. [c] E_t = −728.2164 for $CuH(PH_3)_2$ and −187.8906 for CO_2. [d] E_t = −2318.4639 for $CuH(PH_3)_2$ and −187.5530 for CO_2. [e] E_t = −1034.3067 for $CuH(PH_3)_2$ and −187.1729 for CO_2. [f] E_t = −1068.4747 for $CuH(PH_3)_2$ and −187.1729 for CO_2. [g] E_t = −1069.0617 for $CuH(PH_3)_2$ and −187.8906 for CO_2. [h] E_t = −2506.1075 for $CuH(PH_3)_2$ and −187.5530 for CO_2. The E_t values have hartree units.

Computational Details

MO calculations were carried out with Gaussian 82[24] and IMSPACK[25] programs, where three kinds of basis sets were employed. In the small

(6) (a) Flynn, B. P.; Vaska, L. *J. Chem. Soc., Chem. Commun.* **1974**, 703. (b) Darensbourg, D. J.; Grotsch, G.; Wiegreffe, P.; Rheingold, A. L. *Inorg. Chem.* **1987**, *26*, 3827. (c) Lundquist, E. G.; Folting, K.; Huffman, J. C.; Caulton, K. G. *Inorg. Chem.* **1987**, *26*, 205.
(7) Komiya, S.; Yamamoto, A. *Bull. Chem. Soc. Jpn.* **1976**, *49*, 784.
(8) Darensbourg, D. J.; Pala, M.; Waller, J. *Organometallics* **1983**, *2*, 1285.
(9) (a) Takeda, N.; Inoue, S. *Bull. Chem. Soc. Jpn.* **1978**, *51*, 3564. (b) Aida, T.; Inoue, S. *J. Am. Chem. Soc.* **1983**, *105*, 1304. (c) Kojima, F.; Aida, T.; Inoue, S. *J. Am. Chem. Soc.* **1986**, *108*, 391.
(10) (a) Darensbourg, D. J.; Rokicki, A.; Darensbourg, M. Y. *J. Am. Chem. Soc.* **1981**, *103*, 3223. (b) Darensbourg, D. J.; Rokicki, A. *J. Am. Chem. Soc.* **1982**, *104*, 349. (c) Darensbourg, D. J.; Rokicki, A. *Organometallics* **1982**, *1*, 1685. (d) Tooley, P. A.; Ovalles, C.; Kao, S. C.; Darensbourg, D. J.; Darensbourg, M. Y. *J. Am. Chem. Soc.* **1986**, *108*, 5465. (e) Darensbourg, D. J.; Sanchez, K. M.; Rheingold, A. L. *J. Am. Chem. Soc.* **1987**, *109*, 290.
(11) (a) Darensbourg, D. J.; Grotsch, G. *J. Am. Chem. Soc.* **1985**, *107*, 7473. (b) Darensbourg, D. J.; Hanckel, R. K.; Bauch, C. G.; Pala, M.; Simonons, D.; White, J. N. *J. Am. Chem. Soc.* **1985**, *107*, 7563. (c) Darensbourg, D. J.; Pala, M. *J. Am. Chem. Soc.* **1985**, *107*, 5687. (d) Darensbourg, D. J.; Bauch, C. G.; Rheingold, A. L. *Inorg. Chem.* **1987**, *26*, 977.
(12) (a) Darensbourg, D. J.; Darensbourg, M. Y.; Goh, L. Y.; Ludvig, M.; Wiegreffe, P. *J. Am. Chem. Soc.* **1987**, *109*, 7539. (b) Carmona, E.; Palma, P.; Paneque, M.; Poveda, M. L. *J. Am. Chem. Soc.* **1986**, *108*, 6425.
(13) Buhro, W. E.; Chisholm, M. H.; Folting, K.; Huffman, J. C. *Inorg. Chem.* **1987**, *26*, 3087.
(14) Kato, M.; Ito, T. *Inorg. Chem.* **1985**, *24*, 504; *Inorg. Chem.* **1985**, *24*, 509.
(15) Cocolios, P.; Guilard, R.; Bayeul, D.; Lecomte, C. *Inorg. Chem.* **1985**, *24*, 2058.
(16) (a) Lehn, J.-M.; Ziessel, R. *Proc. Natl. Acad. Sci. U.S.A.* **1982**, *79*, 701. (b) Hawecker, J.; Lehn, J.-M.; Ziessel, R. *J. Chem. Soc., Chem. Commun.* **1985**, 56. (c) Willner, I.; Mandler, D.; Riklin, A. *J. Chem. Soc., Chem. Commun.* **1986**, 1022. (d) Darensbourg, D. J.; Ovalles, C. *J. Am. Chem. Soc.* **1987**, *109*, 3330; *Inorg. Chem.* **1986**, *25*, 1603. (e) Kutal, C.; Corbin, A. J.; Ferraudi, G. *Organometallics* **1987**, *6*, 553. (f) Grant, J. L.; Goswami, K.; Spreer, L. O.; Otvos, J. W.; Calvin, M. *J. Chem. Soc., Dalton Trans.* **1987**, 2105.
(17) For example: (a) Fischer, B.; Eisenberg, R. *J. Am. Chem. Soc.* **1980**, *102*, 7361. (b) Hawecker, J.; Lehn, J.-M.; Ziessel, R. *J. Chem. Soc., Chem. Commun.* **1984**, 328. (c) Beley, M.; Collin, J.-P.; Ruppert, R.; Sauvage, J.-P. *J. Chem. Soc., Chem. Commun.* **1984**, 1315; *J. Am. Chem. Soc.* **1986**, *108*, 7461. (d) Lieber, C. M.; Lewis, N. S. *J. Am. Chem. Soc.* **1984**, *106*, 5033. (e) Ishida, H.; Tanaka, H.; Tanaka, K.; Tanaka, T. *Chem. Lett.* **1987**, 597; *J. Chem. Soc., Chem. Commun.* **1987**, 131; *Chem. Lett.* **1987**, 1035. (f) Ogura, K.; Uchida, H. *J. Chem. Soc., Dalton Trans.* **1987**, 1377 and references therein.
(18) (a) Sakaki, S.; Kudou, N.; Ohyoshi, A. *Inorg. Chem.* **1977**, *16*, 202. (b) Sakaki, S.; Kitaura, K.; Morokuma, K. *Inorg. Chem.* **1982**, *21*, 760. (c) Sakaki, S.; Dedieu, A. *J. Organomet. Chem.* **1986**, *314*, C63. (d) Sakaki, S.; Dedieu, A. *Inorg. Chem.* **1987**, *26*, 3278.
(19) Mealli, C.; Hoffmann, R.; Stockis, A. *Inorg. Chem.* **1984**, *23*, 56.
(20) Ziegler, T. *Inorg. Chem.* **1986**, *25*, 2721.
(21) Branchadell, V.; Dedieu, A. *Inorg. Chem.* **1987**, *26*, 3966.
(22) Sakaki, S.; Ohkubo, K. *Inorg. Chem.* **1987**, *27*, 2020.
(23) CO_2 insertion reactions with $Cu(BH_4)$(triphos), $Cu(PR_3)_2(BH_4)$, and $[CuH(PPh_3)]_4$ have been reported.[4d,5] We examined CO_2 insertion with $CuH(PH_3)_2$ and $CuH(PH_3)_3$ as a model of the insertion into transition-metal alkyl complexes.
(24) Binkley, J. S.; Frisch, M.; DeFrees, D.; Raghavachari, K.; Whiteside, R. A.; Schlegel, H. B.; Pople, J. A. "Gaussian 82", Carnegie-Mellon Chemistry Publishing Unit, Pittsburgh, PA, 1984. Subroutines for effective core potential offered by Dr. P. J. Hay were added by Dr. N. Koga at the Institute for Molecular Science.
(25) Morokuma, K.; Kato, S.; Kitaura, K.; Ohmine, I.; Sakai, S.; Obara, S. "IMSPACK"; IMS Computer Center Library Program, 1980, No. 0382.

basis set (BS I), core orbitals of Cu were replaced by an effective core potential (ECP) given by Hay et al. and its valence orbitals were represented by a (3s 2p 5d) primitive set contracted to a [2s 2p 2d] set.[26] Usual MIDI-3,[27] (4s/2s),[28] and STO-2G[29] sets were used for the CO_2 part, the H ligand, and the PH_3 ligand, respectively. In the medium-size basis set (BS II), the (9s 5p/3s 2p),[28] (4s/3s),[30] and MIDI-3[26] sets were used for the CO_2 part, the H ligand, and the PH_3 ligand, respectively, whereas the same ECP and the same basis set as in the BS I were employed for Cu. In the large basis set (BS III), only a basis set for Cu was changed to a better one, whereas for the other atoms the same basis sets were used as in the BS II: For Cu, the (14s 9p 5d) primitive set of Wachters[31] was augmented with one diffuse d primitive function (ζ = 0.1491) given by Hay[32] and two p primitive functions[31] describing the valence 4p orbitals.[33] A resultant (14s 11p 6d) primitive set was contracted to a [5s 4p 3d] set.[34] All these basis sets were of double-ζ quality for valence orbitals, except that a minimal basis set was used for PH_3 in the BS I and a triple-ζ basis set was used for the Cu 3d orbitals in the BS III set. The BS I set was mainly employed for geometry optimization, and the BS II and BS III sets were used for determining energetics and discussing electronic structure such as bonding nature and electron distribution. MP2 calculations[35] were carried out with the BS II set, because the BS III set is too large for MP2 calculations.

Geometries of reactants (1[36] and CO_2) and products (**2A**, **2B**, **3B**,[37] **4**[38]) were optimized with the energy-gradient method at Hartree–Fock (HF) level (note that **2**, **3**, and **6** have two forms, **A** and **B**; in form **A**, the H atom is close to the Cu atom, but in form **B**, the H atom is distant from the Cu atom, as shown in Figure 1).[39a] The geometry of product **3A** could not be optimized, because it converts to **3B** with no barrier, as will be described later. Nevertheless, MO calculations of **3A** were carried out, to compare this compound with the others such as **2A**, **2B**, and **3B**, where the OCOH group of **3A** was assumed to have the same geometry as in **3B**, as shown in Figure 1. In the reaction system of $CuH(PH_3)_3 + CO_2$, geometry optimization was carried out with parabolic fitting of total energies, because of the big size of this reaction system. In **5**, the Cu–H and Cu–P distances and PCuP angle were optimized independently.[39b] In **6B**[39c] and **7**, several geometrical parameters such as Cu–O and Cu–P distances and OCuP and CuOC angles were optimized,[39b,40]

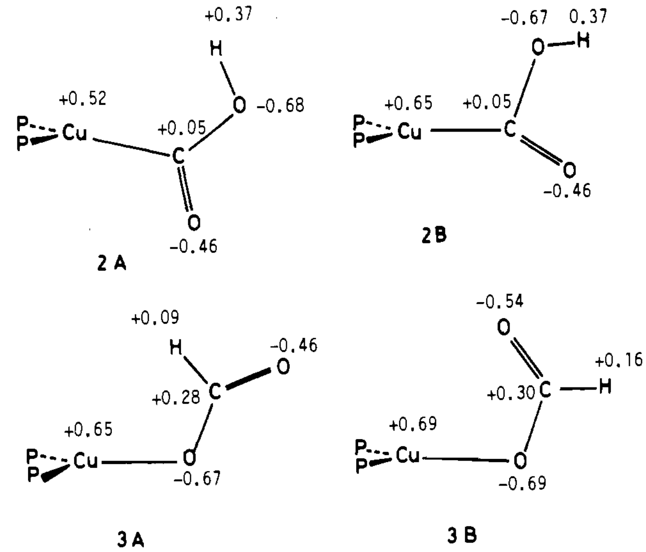

Figure 2. Mulliken charges of $Cu(PH_3)_2(\eta^1\text{-COOH})$ and $Cu(PH_3)_2(\eta^1\text{-OCOH})$. The BS II was used.

Chart II

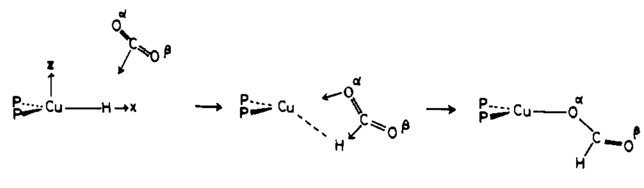

where the geometries of the OCOH and $\eta^2\text{-}O_2CH$ groups were assumed to be the same as in **3B** and **4**, respectively, to save cpu time, because MO calculations of these compounds require much longer cpu time than those of **2**–**4**. Geometry changes caused by CO_2 insertion into a Cu–H bond were also optimized with parabolic fitting of total energies,[39b] as will be described later in detail. In all calculations, the geometry of the PH_3 part was taken from the experimental structure of the PH_3 molecule[41] and fixed during the optimization. These optimized structures are summarized in Figure 1.

Results and Discussion

Relative Stabilities of Products. Relative stabilities of products are given as energy difference from either **1** + CO_2 or **5** + CO_2 in Table I. As clearly seen, **2A** and **2B** are calculated to be much less stable than **3A**, **3B**, and **4**, suggesting that **2A** and **2B** would not be products of the CO_2 insertion (this will be discussed later in more detail). Although **4** is calculated to be slightly less stable than **3B** with the BS II set at the HF level, introduction of electron correlation effect with the MP2 method indicates **3B** and **4** are of nearly the same energy. Furthermore, **4** is calculated to be slightly more stable than **3B** with the larger BS III set at the HF level. Therefore, it is reasonably concluded that **4** is the most stable of these products and probably a final product and that there is a possibility of **3B** being formed as an intermediate, since the difference in stability between **3B** and **4** is very small. When three PH_3 ligands coordinate with Cu, $Cu(PH_3)_3(\eta^1\text{-OCOH})$ (**6B**) is calculated to be more stable than $Cu(PH_3)_3(\eta^2\text{-}O_2CH)$ (**7**), as one might expect from a general fact that a five-coordinate Cu(I) complex is rare. The weakness of the $\eta^2\text{-}O_2CH$ coordination in **7** is clearly shown by the long Cu–O distance of this compound (compare **7** with **4** and **6** in Figure 1). In this case, therefore, **6** is considered a final product. A previous experiment reported that the CO_2 reaction with $Cu(\eta^2\text{-}BH_4)(PR_3)_2$ yields $Cu(PR_3)_2(\eta^2\text{-}O_2CH)$ but the CO_2 reaction with $Cu(\eta^1\text{-}BH_4)(PR_3)_3$ produces $Cu(PR_3)_3(\eta^1\text{-OCOH})$.[5] Thus, the present calculations agree with these experimental results.

(26) Hay, P. J.; Wadt, W. R. *J. Chem. Phys.* **1985**, *82*, 270. Contraction scheme is (21/11/41), where primitive Gaussians are ordered as exponents decrease.
(27) Tatewaki, H.; Hujinaga, S. *J. Comput. Chem.* **1980**, *1*, 205.
(28) Dunning, T. H.; Hay, P. J. In *Methods of Electronic Structure Theory*; Schaefer, H. F., Ed.; Plenum: New York, 1977; p 1.
(29) Hehre, W. J.; Stewart, R. F.; Pople, J. A. *J. Chem. Phys.* **1969**, *51*, 2657.
(30) Dunning, T. H. *J. Chem. Phys.* **1970**, *53*, 2823.
(31) Wachters, A. J. H. *J. Chem. Phys.* **1970**, *52*, 1033.
(32) Hay, P. J. *J. Chem. Phys.* **1977**, *66*, 4377.
(33) Original exponents of Cu 4p orbitals that were optimized for atomic Cu were not used directly but were used after scaling up by a factor of 1.5, to make them more suitable for molecular calculation, according to Wachters.[31]
(34) Contraction scheme is (82211/6311/411), where primitive Gaussians are ordered as exponents decrease.
(35) A frozen-core approximation was applied, where 1s orbitals of C and N and 1s, 2s, and 2p orbitals of P were considered core orbitals (note core orbitals of Cu were replaced by ECP in the BS II).
(36) In the geometry optimization of **1**, the C_{2v} symmetry was assumed. After optimization, distortion from the C_{2v} symmetry was examined by moving the H ligand from the CuP_2 plane, but it destabilized the total energy.
(37) In geometries of **2A**, **2B**, **3A**, and **3B**, the C_s symmetry was taken to minimize the steric repulsion between the COOH or OCOH group and the PH_3 ligand. This seems reasonable, since COOH and OCOH groups are considered to rotate easily around the coordinate bond.
(38) The geometry of **4** was assumed to be C_{2v} symmetry, as shown in Figure 1, since the Cu(I) complex tends to take a tetrahedral-like structure.
(39) (a) The Cu–P bond length and PCuP angle were optimized with parabolic fitting of total energies, after optimizing the Cu–H, Cu–OCOH, Cu–COOH, or $Cu(\eta^2\text{-}O_2CH)$ part with the energy gradient method, to decrease cpu time consumed for gradient calculation. This seems reasonable, because these geometrical parameters change little from compound to compound. (b) All the bond lengths and bond angles were optimized independently, in which optimized values are consistent within 0.02 Å in bond length and 5° in bond angle. (c) **6A** was calculated to be much less stable than **6B**, where the structure of **6A** like **3A** was assumed from the structure of **6B**. Thus, the **6A** was not optimized, since the conversion from **6A** to **6B**, as well as that from **2A** to **2B**, is expected to proceed with a very small barrier.
(40) In the geometry of **6**, the C_s symmetry was taken as in **2A**, **2B**, **3A**, and **3B**. In the geometry of **7**, the $\eta^2\text{-}O_2CH$ rotation around the z axis was examined but the energy change was very small (less than 1 kcal/mol with the BS I set).

(41) Herzberg, G. *Molecular Spectra and Molecular Structure*; D. Van Nostrand Co. Inc.: Princeton, NJ, 1967; p 610.

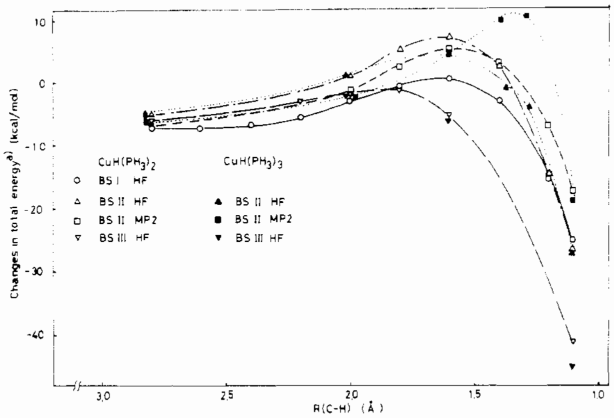

Figure 3. Total energy change[a] caused by CO_2 insertion into a Cu–H bond of $CuH(PH_3)_2$ and $CuH(PH_3)_3$:[b] (a) the infinite separation is taken as a standard (energy change = 0); (b) energy points (HF BS III) of the $CuH(PH_3)_3 + CO_2$ system are not connected by line, because of the lack of their points.

Compared with the reactants (**1** + CO_2), both **3** and **4** are much more stable (see Table I). Also, the product **6** is considerably more stable than the reactants (**5** + CO_2). These results indicate that the CO_2 insertion into a Cu(I)–H bond is significantly exothermic.[42]

We shall now discuss why the M–COOH type complex is less stable than the M–OCOH type complex. Certainly, the M–COOH complex has not been observed experimentally as a product in the CO_2 insertion. The first reason is easily found in electron distribution shown in Figure 2. In **2A** and **2B**, the positively charged $C^{\delta+}$ atom coordinates with the positively charged $Cu^{\delta+}$ atom, whereas in **3A** and **3B** the negatively charged $O^{\delta-}$ atom interacts with the positively charged $Cu^{\delta+}$ atom. Apparently, electrostatic interaction disfavors **2A** and **2B**, but favors **3A** and **3B**. The second reason would be suggested from comparing the C–O bond distance between **2** and **3**. In the M–OCOH type compound **3**, both C–O^α and C–O^β bond lengths are of nearly equal, which would mean that the C–O^α bond strongly conjugates with the C–O^β bond. In the M–COOH type compound **2**, on the other hand, the C–O^α bond is considerably shorter than the C–O^β bond, which indicates that the C–O^α bond is of double-bond character but the C–O^β bond is of single-bond character. This corresponds to very small conjugation between the C–O^α and C–O^β bonds in the M–COOH group. These two factors make the M–COOH type compound less stable than the M–OCOH type compound.

Difference in stability between **3A** and **3B** is also discussed here, because the CO_2 insertion into the Cu(I)–H bond is expected to yield first the less stable **3A**, as shown in Chart II. In **2A** and **3A**, the H atom of the COOH and OCOH groups is positioned near the Cu atom, while in **2B** and **3B**, the H atom is positioned away from the Cu atom. Because both H and Cu atoms are positively charged as shown in Figure 2, electrostatic interaction disfavors **2A** and **3A**. This is probably the main reason that **2A** and **3A** are less stable than **2B** and **3B**. The fact that **6B** is calculated to be more stable than **6A** can be rationalized in a similar way.

(42) (a) The calculated exothermicity much depends on the kinds of basis sets and the inclusion of electron correlation effect. However, all types of calculations indicate the significance of exothermicity. Thus, it is reasonably concluded that the CO_2 insertion into a Cu(I)–H bond is exothermic. (b) In the BS II, the ECP is used for core orbitals of Cu and the Cu 3d orbital is of double-ζ quality. In the BS III, an all-electron basis set is used for Cu and the Cu 3d orbital is of triple-ζ quality. To investigate what factor gives rise to the significant basis set effect, **1** and **3A** were calculated with the modified BS III set in which only the basis set for Cu was changed to a (82211/6311/51) contracted set,[31,32] i.e., the double-ζ quality for the Cu 3d orbital. Both total energies of **1** and **3A** decrease by only 0.0024 hartree upon going to the modified BS III set from the BS III set. Therefore, the exothermicity little changes through the modification of BS III. These results suggest that the significant basis set effect comes from the different representation of core orbitals, either use of ECP or use of all-electron basis sets. More detailed investigation of the basis set and correlation effects is in progress now.

Table II. Comparison of the $CuH(PH_3)_2 + CO_2$ Reaction System with the $CuH(PH_3)_3 + CO_2$ Reaction System (kcal/mol for ΔE_{act})

		$CuH(PH_3)_2$		$CuH(PH_3)_3$	
basis set	method	R(C–H)	ΔE_{act}[a]	R(C–H)	ΔE_{act}[b]
BS I	HF	1.6	7.8	1.6	5.1
BS II	HF	1.6	12.5	1.6	8.0
	HF (with BSSE cor)	1.6	16.1		
	MP2	1.6	12.9	1.3	18.0
BS III	HF	1.8	5.4		
		(2.0	4.7)	2.0	2.5

Changes in Mulliken Population[c] (BS III Used; R(C–H) = 2.0 Å)

	$CuH(PH_3)_2$	$CuH(PH_3)_3$		$CuH(PH_3)_2$	$CuH(PH_3)_3$
Cu	−0.215	−0.307	C	0.027	0.035
PH_3	−0.001	0.012	O	0.077	0.076
H ligand	0.109	0.137	O	0.006	0.024
CO_2	0.110	0.136			

[a] The activation barrier was approximately estimated as an energy difference from the total energy of the reaction system at R(C–H) = 2.8 Å.[44] [b] Because many points were not calculated in this reaction system, the energy difference was estimated at the same R(C–H) distance. Of course, the reaction system is the most unstable at this R(C–H) distance. [c] The standard (change 0) is taken for the infinite separation.

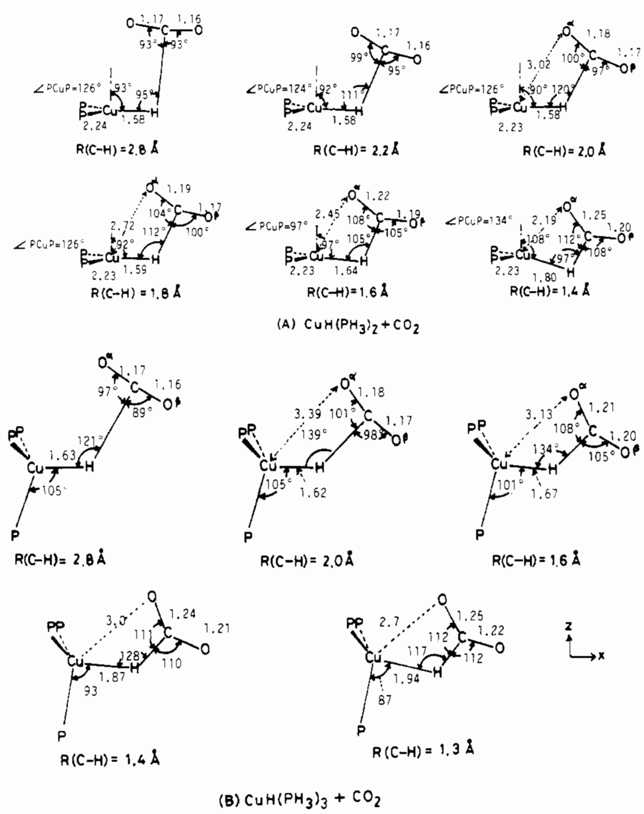

Figure 4. Geometry change caused by CO_2 insertion into a Cu–H bond of $CuH(PH_3)_2$ and $CuH(PH_3)_3$.

CO_2 Insertion into a Cu–H bond of $CuH(PH_3)_2$ and $CuH(PH_3)_3$. In the reaction between $CuH(PH_3)_2$ and CO_2, **3B** and **4**, which are predicted to be the intermediate and the product, respectively, hold a C–H bond newly formed between the H ligand of $CuH(PH_3)_2$ and C of CO_2. Therefore, the distance R(C–H) between H of $CuH(PH_3)_2$ and C of CO_2 was taken as a reaction coordinate, and changes in geometry and total energies by the CO_2 insertion were investigated, where the Cu–H, C–O^α, C–O^β, and Cu–P distances and zCuH (z = z axis), CuHC, HCO^α, and HCO^β angles were optimized independently (see Chart II).[43] Total energy

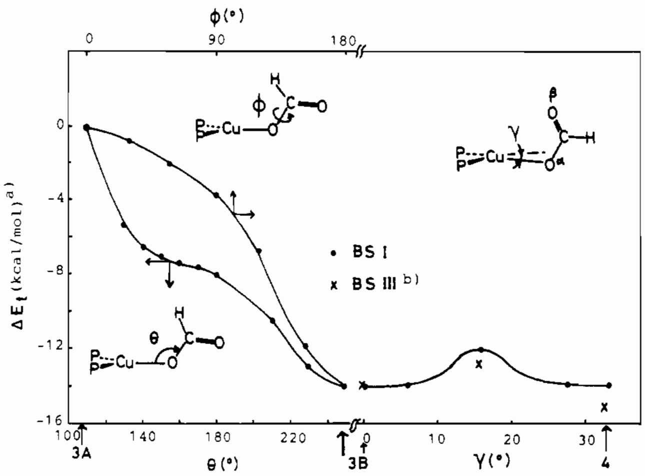

Figure 5. Total energy change caused by conversion from $Cu(PH_3)_2(\eta^1\text{-OCOH})$ (**3A**) to $Cu(PH_3)_2(\eta^2\text{-}O_2CH)$ (**4**): (a) the standard (energy 0) is taken for the total energy of **3A**; (b) the total energy of **3B** calculated with BS III is placed at the same level as the total energy of **3B** calculated with BS I.

changes obtained with various basis sets are shown as a function of R(C–H) in Figure 3, and activation barriers are summarized in Table II.[44] The similar values of activation barrier are calculated with the BS I and BS II (ECP calculations) at the HF level. Introduction of the electron correlation effect with the MP2 method changes little the activation barrier. The basis set superposition error (BSSE) was estimated with the method of Boys and Barnardi[45] at R(C–H) = 1.6–2.0 Å. The correction of BSSE somewhat increases the activation barrier by ca. 3.6 kcal/mol (at R(C–H) = 1.6 Å) but has little influence on the position of transition state.[46] However, the use of BS III (all-electron calculation) considerably lowers the activation barrier and shifts the position of transition state to the early stage of the reaction. In either event, the activation barrier of the CO_2 insertion is estimated to be rather low.

Geometry changes are displayed in Figure 4A. As the CO_2 insertion into the Cu–H bond proceeds, the geometry of the reaction system becomes similar to that of $Cu(PH_3)_2(\eta^1\text{-OCOH})$ (**3A**). However, this compound is not a final product and **3B** is calculated to be more stable than **3A**. Two kinds of conversion paths from **3A** to **3B** were examined; in the first, the $CuO^{\alpha}C$ angle was taken as a reaction coordinate, and in the second, the rotation around the $C\text{–}O^{\alpha}$ bond was taken as a reaction coordinate (the geometry of the OCOH group was not optimized but fixed during this conversion). As shown in Figure 5, the total energy decreases monotonously upon going to **3B** from **3A**.[47] Although it is difficult

Chart III

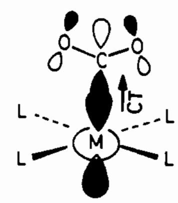

to determine which conversion path is more plausible, it is safely concluded that **3A** converts to **3B** with no barrier.

Because **4** is the final product, the isomerization from **3B** to **4** was examined with the BS I set, where a γ angle was taken as a reaction coordinate (see Figure 5 for the γ angle). In this geometry change, the $CuO^{\alpha}C$ angle and the $Cu\text{–}O^{\alpha}$ distance were optimized with parabolic fitting of total energies, while the other geometrical parameters were assumed by linear-transit approximation, because they vary only slightly upon going from **3B** to **4**. The calculated activation barrier is very small (much smaller than the barrier from **1** to **3A**). Thus, the isomerization from **3A** to the final product **4** does not seem to be a rate-determining step. On the other hand, the CO_2 insertion step yielding **3A** seems the most important in this reaction, because this step involves the highest activation barrier and the CO_2 insertion can be viewed to be completed at **3A**.

In the CO_2 insertion reaction with $CuH(PH_3)_3$, the final product, $Cu(PH_3)_3(\eta^1\text{-OCOH})$ (**6B**), also involves a newly formed C–H bond. The R(C–H) distance between C of CO_2 and H of $CuH(PH_3)_3$ was therefore taken as a reaction coordinate, again. Because this reaction system is large and geometry optimization needs a lot of cpu time, only a few of points of the reaction path were optimized, as shown in Figures 3 and 4B. On the HF level, the total energy changes of this reaction system much resemble those of the $CuH(PH_3)_2 + CO_2$ reaction system, except that the activation barrier of this reaction system is slightly lower than that of the reaction system of $CuH(PH_3)_2 + CO_2$, as compared in Table II. On the other hand, MP2 calculations indicate that this reaction system exhibits the higher activation barrier and later transition state than the $CuH(PH_3)_2$ reaction system. This discrepancy between HF and MP2 calculations makes quantitative discussion difficult, and further detailed investigation including electron correlation effect would be necessary. In any event, geometry changes found in this reaction system much resemble those found in the $CuH(PH_3)_2 + CO_2$ reaction system (see Figure 4), except that the CuHC angle of this reaction system is larger than that of the $CuH(PH_3)_2$ reaction system. All these results will be discussed later in more detail.

Changes in Electron Distribution and Bonding Nature during the CO_2 Insertion. Since the reaction steps yielding **3A** and **6A** seem important, as described above, they will be examined in more detail. Around the transition state of the $CuH(PH_3)_2 + CO_2$ reaction system [R(C–H) = 1.6–2.0 Å], the $CuH(PH_3)_2$ moiety is little distorted, but the CO_2 moiety is distorted somewhat, as shown in Figure 4. It is also noted that the O^{α} atom of CO_2 is approaching the Cu atom around the transition state.

Mulliken populations, shown in Figure 6, exhibit several interesting changes in electron distribution during the reaction: (1) The electron population of the H ligand increases with approach of CO_2 to $CuH(PH_3)_n$, attaining a maximum at R(C–H) = 2.0 Å and then decreasing gradually, (2) the electron population of the CO_2 moiety increases as CO_2 approaches $CuH(PH_3)_n$, and (3) the electron population of the O^{α} atom increases more than that of the O^{β} atom.

The first result shows that the polarization in the $CuH(PH_3)_n$ part occurs at a rather early stage of the reaction, through which electrons of the $CuH(PH_3)_n$ moiety are withdrawn toward the Lewis acid center of CO_2. This electron flow leads to an increase in the electrostatic attraction between the H ligand and the C atom of CO_2, and at the same time, this would be a preparation of charge-transfer interaction from $CuH(PH_3)_n$ to CO_2, which would become important on the later stage of the reaction, as described below.

(43) The C_s symmetry was assumed in the optimization. This assumption seems reasonable, by considering that Cu(I) tends to form a tetrahedral-like four-coordinate structure (see Chart II). The deviation from the C_s symmetry was examined in two ways; in the first, the CO_2 moiety was rotated around the C–H bond, and in the second, the CO_2 moiety was rotated around the Cu–H bond. Both deviations were calculated to destabilize the reaction system (the BS I was used).

(44) The activation barrier was estimated as an energy difference from the reaction system at R(C–H) = 2.8 Å. These values were rather arbitrarily estimated, but they seem reasonable, because the reaction system at R(C–H) = 2.8 Å has almost the same structure as at infinite separation and its total energy little changes upon going to R(C–H) = 2.6 Å from R(C–H) = 2.8 Å.

(45) Boys, S. F.; Bernardi, F. *Mol. Phys.* **1970**, *19*, 553. Ostlund, N. S.; Merrifield, D. L. *Chem. Phys. Lett.* **1976**, *39*, 612.

(46) BSSE was calculated to be 2.8 kcal/mol at R(C–H) = 2.0 Å and 3.2 kcal/mol at R(C–H) = 1.8 Å with the BS II set. The position of the transition state is hardly influenced by taking into account BSSE.

(47) A careful inspection of the lower curve of Figure 5 suggests that possibility that the secondary minimum exists around θ = 160°. However, the BS I calculations indicate that the minimum would be very shallow, even if it existed. Better calculations would be expected not to deepen the minimum, because the energy difference between **3A** and **3B** depends little on the kind of basis sets and inclusion of the electron correlation effect. Thus, it is safely concluded that the conversion from **3A** to **3B** is facile.

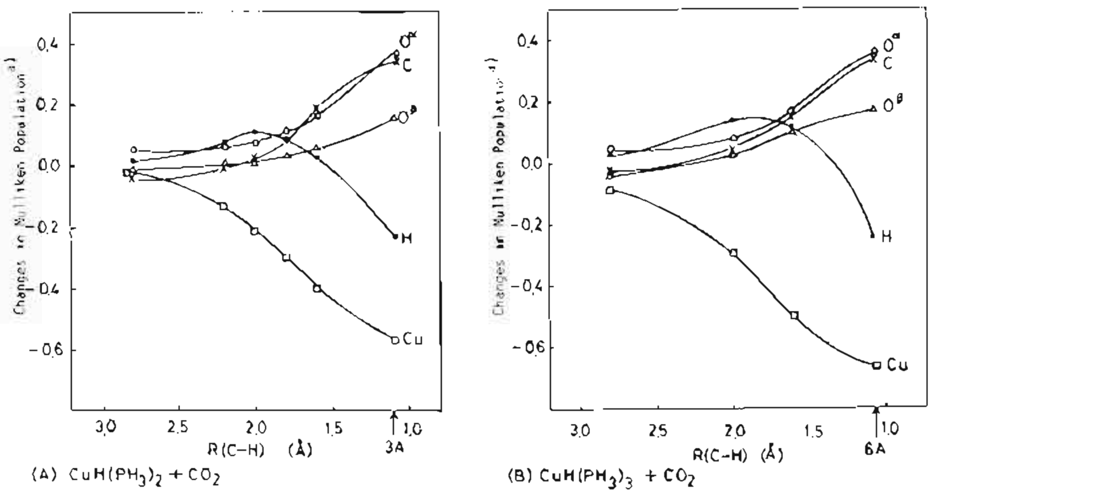

Figure 6. Changes in Mulliken populations caused by CO_2 insertion into a Cu-H bond of $CuH(PH_3)_2$ or $CuH(PH_3)_3$ (BS III) used: (a) the infinite separation is taken as a standard.

Chart IV

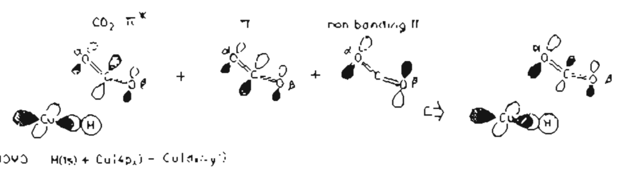

Chart V

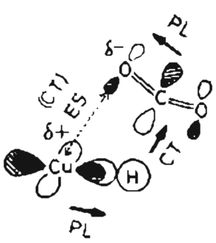

The second result clearly indicates that the charge-transfer interaction from $CuH(PH_3)_n$ to CO_2 becomes stronger, as the CO_2 insertion proceeds. The importance of this kind of charge-transfer interaction is quite the same as in the η^1-C-coordinated CO_2 complexes of $[Co(alen)_2(CO_2)]^-$ (alen = $HNCHCHCHO^-$) and $RhCl(AsH_3)_4(CO_2)$, in which the σ type charge-transfer interaction from the metal part to CO_2 π^* orbital is of primary importance (see Chart III), as has been demonstrated by recent ab initio MO studies.[18d,48] In these CO_2 complexes, the η^1-C-coordinated CO_2 is significantly distorted, which pushes down the CO_2 π^* orbital energy and, as a result, strengthens the charge-transfer interaction from metal to CO_2. In the present reaction systems, the CO_2 distortion increases as the insertion reaction proceeds. Thus, as well as in the η^1-C-coordinated CO_2 complexes, the CO_2 distortion in the present reaction systems indicates that the charge-transfer interaction from the metal part to CO_2 is important in the CO_2 insertion reaction.

The third result is not caused by a simple charge-transfer interaction from $CuH(PH_3)_n$ to the CO_2 π^* orbital, because the simple charge-transfer interaction equally increases both electron populations of O^{α} and O^{β} atoms. Several orbital mixings, shown in Chart IV, take place in this reaction system; the main part is the HOMO–LUMO interaction between the HOMO of $CuH(PH_3)_n$ and LUMO of CO_2 (π^* orbital). Into this HOMO–LUMO overlap, the CO_2 π orbital mixes in an antibonding fashion with the HOMO of $CuH(PH_3)_2$, in quite the same fashion as in the η^1-C-coordinated CO_2 complex,[48] with which the electron population is accumulated on the O atom but reduced from the C atom. If this mixing does not occur, the electron population of the C atom increases much more than that of the O atom, since the CO_2 π^* orbital has the larger p_{π} lobe on the C atom compared to that on the O atom. Further mixing of the CO_2 nonbonding π orbital is induced by the positively charged $Cu^{\delta+}$ atom through the static orbital mixing,[49] because the O^{α} atom is closer to the $Cu^{\delta+}$ atom than the O^{β} atom is. This makes the O^{α} electron population larger than that of the O^{β} atom. The resultant large negative charge on the O^{α} atom stabilizes the reaction system by electrostatic attraction between $Cu^{\delta+}$ and $(O^{\alpha})^{\delta-}$ atoms. The enlarged p_{π} orbital of the O^{α} atom would be of use for donative interaction from the O^{α} atom to the Cu atom. Although the energetical contribution of this interaction is not significant around the transition state (see the small value of CTPLXB in Table III), this interaction would lead to the coordinate bond of the OCOH group in the late stage of the reaction.[50a]

All these features that are common in both reaction systems of $CuH(PH_3)_2$ and $CuH(PH_3)_3$ are summarized in Chart V. It follows from this chart that CO_2 interacts with the H ligand through the charge-transfer interaction from the H ligand to CO_2 and the electrostatic interaction between the $Cu^{\delta+}$ and $(O^{\alpha})^{\delta-}$ atoms. Additionally, the charge-transfer interaction from O^{α} to Cu contributes to the Cu–O^{α} bond formation in the late stage of the reaction.[50] These interactions correspond to a four-center-like transition state,[50c] which agrees well with the proposals in several experimental works.[5,10a,c]

The interaction between $CuH(PH_3)_n$ and CO_2 is investigated at rather early stage of the reaction with energy decomposition analysis.[51] In Table III, ΔE_t is the stabilization energy of the reaction system compared to the reactants of $CuH(PH_3)_n$ and CO_2, which take equilibrium structures, DEF (deformation energy) is the destabilization energy required to distort $CuH(PH_3)_n$ and CO_2 from their equilibrium structures to the distorted ones in the reaction system, and INT (interaction energy) is the stabilization energy compared to $CuH(PH_3)_n$ and CO_2, which are distorted as in the reaction system. This INT is divided into several

(48) Sakaki, S.; Aizawa, T.; Koga, N.; Morokuma, K.; Ohkubo, K. *Inorg. Chem.* **1989**, *28*, 103.
(49) Imamura, A.; Hirano, T. *J. Am. Chem. Soc.* **1975**, *97*, 4192.

(50) (a) The electron density accumulation, which results from the charge-transfer interaction from O^{α} to Cu, is clearly demonstrated in the later stage of the CO_2 insertion into the Cu–CH_3 bond. (Sakaki, S. To be published.) (b) The long Cu–O^{α} distance of the $CuH(PH_3)_3$ + CO_2 system suggests that the Cu–O^{α} coordinate bond would be formed at a late step of the reaction, probably at R(C–H) < 1.3 Å (see Figure 4). (c) The $CuH(PH_3)_3$ + CO_2 system has a longer Cu–O^{α} distance at every reaction step than the $CuH(PH_3)_2$ + CO_2 system does. However, the fact that the O^{α} atomic population is larger than the O^{β} atomic population suggests the presence of the electrostatic attraction between Cu and O^{α} atoms. Thus, the four-center-like transition state cannot be neglected even in the $CuH(PH_3)_3$ reaction system, in spite of the long Cu–O^{α} distance.

(51) (a) Morokuma, K. *Acc. Chem. Res.* **1977**, *10*, 294. (b) Kitaura, K.; Morokuma, K. *Int. J. Quant. Chem.* **1976**, *10*, 325. (c) Kitaura, K.; Sakaki, S.; Morokuma, K. *Inorg. Chem.* **1981**, *20*, 2292.

chemically meaningful terms, as follows: INT = ES + EX + CTPLXA($CuHP_n \rightarrow CO_2$) + CTPLXB($CO_2 \rightarrow CuHP_n$) + R, where P means PH_3, ES and EX are the electrostatic (Coulombic) interaction and the exchange repulsion interaction between $CuH(PH_3)_n$ and CO_2, respectively, CTPLXA involves the charge transfer from $CuH(PH_3)_n$ to CO_2, polarization of CO_2, and their coupling terms, CTPLXB involves the charge transfer from CO_2 to $CuH(PH_3)_n$, polarization of $CuH(PH_3)_n$, and their coupling terms, and R is the higher order remaining term (note that negative values mean stabilization for all the terms). At long separation (R(C–H) = 2.8 Å) between $CuH(PH_3)_n$ and CO_2, the ES stabilization is larger than the EX destabilization, as shown in Table III. Both charge-transfer type interactions, CTPLXA and CTPLXB, however, exhibit small stabilization. These features suggest the importance of the ES interaction at long separation, as one might usually expect. When CO_2 approaches $CuH(PH_3)_n$ (for instance R(C–H) = 2.0 Å), the EX destabilization overwhelms the ES stabilization. This net destabilization in the static interaction (sum of ES and EX) is compensated by the increased stabilization of CTPLXA($CuHP_n \rightarrow CO_2$). The stabilization of CTPLXB($CO_2 \rightarrow CuHP_n$) is remarkably small. These results indicate that the charge transfer from $CuH(PH_3)_n$ to CO_2 is important for stabilizing the reaction system, which agrees well with the increase in the CO_2 electron population (vide supra). The DEF of the CO_2 moiety is also one of factors for destabilizing the reaction system, because this value is much larger than the DEF of the $CuH(PH_3)_n$ moiety and is a main part of the total DEF value. From these results, a reasonable picture might appear about the CO_2 insertion: (1) the origin of the activation barrier is the deformation of the CO_2 part and the exchange repulsion between $CuH(PH_3)_n$ and CO_2, and (2) the charge transfer from $CuH(PH_3)_n$ to CO_2 is important for stabilizing the reaction system.

Now, it is worthwhile to compare the reaction system of $CuH(PH_3)_3 + CO_2$ with the reaction system of $CuH(PH_3)_2 + CO_2$. At the early stage of the reaction (R(C–H) = 2.0 Å), the DEF destabilization is slightly larger in the $CuH(PH_3)_3 + CO_2$ system than in the $CuH(PH_3)_2 + CO_2$ system, but at the same time, the INT stabilization is larger in the $CuH(PH_3)_3$ system than in the $CuH(PH_3)_2 + CO_2$ system (see Table III). Consequently, the $CuH(PH_3)_3 + CO_2$ system is less destabilized than the $CuH(PH_3)_2 + CO_2$ system, as shown in Figure 3. The larger stabilization of INT in the $CuH(PH_3)_3 + CO_2$ system comes from the smaller destabilization of static interaction (sum of ES and EX) and slightly larger CTPLXA stabilization. The approaching angle of CO_2 (∠CuHC) in the $CuH(PH_3)_3 + CO_2$ system is larger than in the $CuH(PH_3)_2 + CO_2$ system (see Figure 4). This would decrease the EX repulsion. One of the reasons for this larger approaching angle would be the steric repulsion between CO_2 and three PH_3 ligands; if the approaching angle of the $CuH(PH_3)_3 + CO_2$ system is the same as in the $CuH(PH_3)_2 + CO_2$ system, the former suffers from larger steric repulsion, since this system has one more PH_3 ligand than the $CuH(PH_3)_2$ system. The larger CTPLXA stabilization is consistent with the larger increase of CO_2 electron population in the $CuH(PH_3)_3 + CO_2$ system than in the $CuH(PH_3)_2 + CO_2$ system (see Table II). The Cu electron population decreases more in the $CuH(PH_3)_3 + CO_2$ system upon CO_2 insertion than in the $CuH(PH_3)_2 + CO_2$ system, and at the same time, the electron population of the H ligand increases more around R(C–H) = 2.0 Å than in the latter. These results suggest that the presence of three PH_3 ligands would push up the Cu d orbital energy, enhance the electron flow to the H ligand from Cu, and strengthen the charge-transfer interaction from $CuH(PH_3)_3$ to CO_2. Consequently, CO_2 more easily approaches $CuH(PH_3)_3$ in an early stage of the reaction than it approaches $CuH(PH_3)_2$.

At the later stage of the reaction, it is not easy to compare these two reaction systems, because the results on the MP2 level differ much from the results on the HF level and the results of the $CuH(PH_3)_2 + CO_2$ system; although similar potential curves are given by the HF and MP2 calculations in the $CuH(PH_3)_2 + CO_2$ system, MP2 calculations of the $CuH(PH_3)_3$ reaction system exhibit the higher activation barrier than the activation barrier on the HF level and the activation barrier of the $CuH(PH_3)_2$ system (see Table II). Several factors to be examined are remaining,[52a] and therefore, we shall stop to compare these two reaction systems in detail. Here, we only point out what factor makes a distinction between the $CuH(PH_3)_3$ and $CuH(PH_3)_2$ reaction systems. In the former, three PH_3 ligands push up the Cu d orbital energy, which enhances the charge-transfer interaction from $CuH(PH_3)_n$ to CO_2, as described above. At the same time, three PH_3 ligands suppress the approach of O^α to Cu, as clearly shown by the long Cu–O^α distance around R(C–H) = 1.6–1.3 Å, which retards the formation of the Cu–O^α interaction. If the favorable condition of charge-transfer interaction overwhelms the unfavorable condition of the Cu–O^α interaction, the activation barrier of the $CuH(PH_3)_3$ system becomes smaller than that of the $CuH(PH_3)_2$ system. This situation can be observed at the early stage of the reaction (vide infra). If the steric repulsion of three PH_3 ligands is large, the $CuH(PH_3)_3$ system exhibits a higher activation barrier and a later transition state than the $CuH(PH_3)_2$ system.[52c] In this case, the steric repulsion with three PH_3 ligands would be one of the origins of the activation barrier. These discussions suggest that the small and donative ligand accelerates the CO_2 insertion but the large and less donative ligand suppresses the CO_2 insertion.

What Type of a Metal Complex Easily Undergoes CO_2 Insertion? Summarizing the above discussion, a charge-transfer interaction from the metal complex to CO_2 is of primary importance

(52) (a) The first is the appropriateness of the ECP in MP2 calculations. In the calculations including the electron correlation effect, use of a good and flexible basis set is necessary. The ECP of Cu is probably less flexible than the all-electron basis set. While the MP2 calculations with the BS III set are expected to yield more reliable results, such calculation is much time consuming. The second is the electron correlation effect on geometry. At R(C–H) = 1.4 Å, the C–O^α distance is still long, probably owing to the steric repulsion with three PH_3 ligands. Geometry optimization beyond the HF level is desirable to get more reliable results, since the electron correlation tends to shorten a distance of a weak coordinate bond. The third is the optimization of limited geometrical parameters. For instance, three Cu–P distances and three (x)CuP angles (see Figure 4 for the x axis) were assumed to be the same, but the Cu–P bonds near CO_2 are expected to be pushed away by the approaching CO_2. The fourth is the concerted character of the reaction; in the $CuH(PH_3)_3 + CO_2$ system, the approach of O^α to Cu is suppressed by three PH_3 ligands, which corresponds to the small concerted character. In the $CuH(PH_3)_2 + CO_2$ system, on the other hand, the reaction would be sufficiently concerted, since the approach of O^α to Cu is not suppressed by two PH_3 ligands (see Figure 4A).[52b] Examination of all these factors is not easy, because of the big size of the $CuH(PH_3)_3 + CO_2$ system. (b) Of those factors described in ref 52a, we guess that the fourth factor is important, because the only clear difference in structure between the $CuH(PH_3)_3 + CO_2$ and $CuH(PH_3)_2 + CO_2$ systems is that the former has much longer Cu–O^α distance than the latter. We can easily understand how the difference in the Cu–O distance results in different features of MP2 calculations.[50c] (c) Our preliminary SD-CI calculation of the Cu–CH_3 + CO_2 system[52d] indicates that the CO_2 $n\pi \rightarrow \pi^*$ excited configurations are important in the reactant side (C_0 = 0.93 and $C_{n\pi \rightarrow p^*}$ = 0.08 at 50-Å separation between Cu–CH_3 and CO_2), but the excitation originating from the Cu–O bond is less important in a product of Cu–$OCOCH_3$ (C = ca. 0.03 for this excitation). As the CO_2 insertion proceeds, the C=O double-bond character decreases and the (CO_2 $n\pi \rightarrow \pi^*$) excited configuration becomes small, which suggests that the energy improvement by introducing the electron correlation effect would decrease. This suggestion is supported by the fact that introducing the electron correlation effect decreases exothermicity of the CO_2 insertion (see Table I). In the $CuH(PH_3)_2 + CO_2$ system, the approach of O^α to Cu is not suppressed by two PH_3 ligands (see Figure 4A), and therefore, the Cu–O^α interaction is easily formed in a concerted manner. The increased stabilization by this newly formed Cu–O^α interaction would compensate the decrease in energy improvement induced by introducing an electron correlation effect around the transition state. In the $CuH(PH_3)_3 + CO_2$ system, however, three PH_3 ligands suppress the approach of O^α to Cu and the formation of the Cu–O^α interaction is delayed until the late step of the reaction,[50b] which means the decrease in energy improvement induced by introducing the electron correlation effect is not effectively compensated by the Cu–O^α interaction. This would increase the activation barrier on the MP2 level. More detailed study of the electron correlation effect is in progress now, on a model system. (d) Limited SD-CI calculations of the Cu–CH_3 + CO_2 system were carried out with the MELD program (McMurchie, L.; Elbert, S.; Langhoff, S.; Davidson, E. R. "MELD"; IMS Computer Center Library, No. 030). The double-ζ basis set was used for Cu (contraction 3 of ref 31), and (9s 5p/3s 2p) sets were used for C and O atoms.

Table III. Energy Decomposition Analysis of an Interaction between CO_2 and $CuH(PH_3)_n$ (n = 2, 3)[a]

R(C–H), Å	ΔE_t[b]	DEF[c] tot.	DEF[c] $CuH(PH_3)_n$	DEF[c] CO_2	INT[d]	ES	EX	CTPLXA ($CuHP_n \rightarrow CO_2$)	CTPLXB ($CO_2 \rightarrow CuHP_n$)	R
			(1) $CuH(PH_3)_2 + CO_2$ Yielding $Cu(PH_3)_2(\eta^1\text{-OCOH})$ (3) (C Attack)							
2.8	–4.9	0.7	0	0.7	–5.6	–11.8	9.3	–1.7	–0.9	–0.5
2.0	–0.2	6.6	0.8	5.8	–6.8	–32.4	39.8	–10.5	–2.7	–1.0
1.8	0.5	13.4	0.9	12.5	–12.9	–53.9	74.1	–23.8	–5.0	–4.3
			(2) $CuH(PH_3)_3 + CO_2$ Yielding $Cu(PH_3)_3(\eta^1\text{-OCOH})$ (6)							
2.8	–4.8	0.7	0	0.7	–5.5	–8.3	5.4	–1.7	–0.5	–0.4
2.0	–2.4	7.2	0	7.2	–9.6	–29.1	34.8	–11.3	–2.7	–1.3
			(3) $CuH(PH_3)_2 + CO_2$ Yielding $Cu(PH_3)_2(\eta^1\text{-COOH})$ (2) (O Attack)							
2.0 (100°)[e]	26.0	6.6	0.8	5.8	19.3	–16.0	40.7	–3.2	–2.2	0.3
2.0 (120°)	26.4	6.6	0.8	5.8	19.8	–8.9	33.7	–3.1	–2.0	0.1

[a] Energy units in kcal/mol; negative values mean stabilization. The BS III was used. [b] ΔE_t = the stabilization energy of the reaction system compared to the reactants $CuH(PH_3)_n$ and CO_2, which take equilibrium structures. [c] DEF = the destabilization energy required to distort $CuH(PH_3)_n$ and CO_2 from their equilibrium structures to distorted ones in the reaction system. [d] INT = the stabilization energy of the reaction system compared to $CuH(PH_3)_n$ and CO_2, which are distorted as in the reaction system. [e] The $CuHO^{\alpha}$ angle is in parentheses.

Chart VI

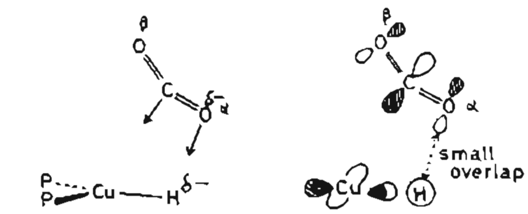

(A) Electrostatic interaction (B) Charge transfer interaction

O-Attack reaction

in the CO_2 insertion. The presence of donating ligand, therefore, favors the insertion, since it strengthens the charge-transfer interaction. If the donating ability of the metal complex is strong enough, the strong charge-transfer interaction can be formed with CO_2 being less distorted. This means the activation barrier becomes small, because the DEF of CO_2 is one of origins of the activation barrier and the strong charge-transfer interaction stabilizes the reaction system. Metal complexes that easily cause the CO_2 insertion satisfy this condition; for instance, Al(imidazole)(porphyrinato)(OR) easily undergoes the CO_2 insertion to form Al(imidazole)(porphyrinato)(OCOOR).[9] Because the OR^- ligand has a lone-pair orbital that is not used for coordination with Al, a charge-transfer interaction from the OR^- to CO_2 is easily formed. Furthermore, the porphyrin can be viewed as an electron pool and the imidazole ligand is electron donating. All these facts indicate Al(imidazole)(porphyrinato)(OR) can form a strong charge-transfer interaction with CO_2. Also, CO_2 insertion with $[MH(CO)_5]^-$ (M = Cr, Mo, W),[10,11] $[HRu_3(CO)_{11}]^-$, and $[(CH_3)Ru_3(CO)_{11}]^-$[8] has been reported by Darensbourg et al. Because these complexes are anionic and probably the negative charge is highly localized on the H and CH_3 ligands, charge transfer from these ligands to CO_2 is considered to occur very easily.

As already mentioned above, the importance of the charge-transfer interaction from the metal part to CO_2 is demonstrated theoretically and experimentally. The degree of the charge-transfer interaction from a metal complex to CO_2 is, therefore, one of the useful guidelines to find a metal complex that easily causes the CO_2 insertion reaction.

Why Is the M–COOH Type Complex Not Formed in the CO_2 Insertion into an M–H Bond? Although the M–COOH type compound, **2**, is predicted not to be a product, a possibility that **2** is formed as an intermediate in the CO_2 insertion still remains. To certify that **2** is not involved as an intermediate, the reaction system yielding **2** (see Chart VI: hereafter called the O attack) is compared with the reaction system yielding 3A (see Chart II: called the C attack) in Table III. In the O attack system, both geometries of $CuH(PH_3)_2$ and CO_2 were assumed to be the same as in the C attack at R(C–H) = 2.0 Å, and the $HO^{\alpha}C$ angle was taken to be the same as the HCO^{α} angle of the C attack system.[53a] EDA results of Table III clearly show the critical difference between the C attack and O attack; the O attack receives much smaller stabilization from the ES and CTPLXA terms than the C attack does.[53b] The smaller ES stabilization would result from the electrostatic repulsion between $Cu^{\delta+}$ and $C^{\delta+}$ atoms (see Chart VIA). The smaller CTPLXA stabilization would arise from the fact that the CO_2 π^* orbital (LUMO) poorly overlaps with the HOMO of $CuH(PH_3)_2$ (see Chart VIB), because the CO_2 π^* orbital consists of the small p_x lobes of the O atom and the large p_x lobe on the C atom. In the C attack, these unfavorable situations disappear; the $C^{\delta+}$ and $O^{\delta-}$ of CO_2 approach the $H^{\delta-}$ ligand and the $Cu^{\delta+}$ atom, respectively, and the CO_2 π^* orbital overlaps well with the HOMO of $CuH(PH_3)_2$, as shown in Chart IV (note that the large C p_x lobe can interact with the HOMO of $CuH(PH_3)_2$, in the C attack). Thus, it would be reasonably concluded that the formation of the M–COOH type compound is very difficult in the CO_2 insertion.

Conclusion

The present theoretical study provides clear features about geometry change, electronic structure, and bonding nature of CO_2 insertion into the Cu(I)–H bond. The most important interaction for accelerating the CO_2 insertion is the charge-transfer interaction from metal complex to CO_2. Almost all complexes that have been reported to undergo easily the CO_2 insertion reaction can form strong charge-transfer interaction with CO_2. Therefore, the strength of the charge-transfer interaction can be used as a guideline to finding a good metal complex capable of proceeding with the CO_2 insertion reaction.

Acknowledgment. S.S. thanks Prof. K. Morokuma for his generous support of this work. S.S. is grateful for financial support from the Ministry of Education, Science, and Culture of Japan through a Grant-in-Aid for Co-operative Research (No. 6303002). Calculations were carried out with Hitac M-680 and S-820 computers at the Computer Center of the Institute for Molecular Science.

(53) (a) To certify that **2** cannot be formed as an intermediate, we must compare the reaction course of the O attack with that of the C attack. Unfortunately, we failed to find the reaction course of the O attack in which the distance between the H ligand and O^{α} of CO_2 was taken as a reaction coordinate. This is probably because the electrostatic repulsion between $C^{\delta+}$ and $Cu^{\delta+}$ does not allow the approach of C to Cu. To find the reaction course of the O attack, at least both R(O–H) and R(Cu–C) must be taken as reaction coordinates. Those calculations are much time consuming and were stopped in the present work. (b) Although the geometry of the O attack was assumed rather arbitrarily, the EDA results are not changed very much upon increasing the $HO^{\alpha}C$ angle from 100 to 120°. Thus, the discussion presented seems reasonable, at least semiquantitatively.